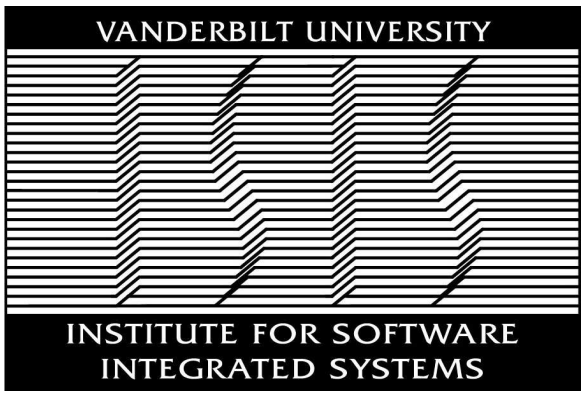

Institute for Software Integrated Systems
Vanderbilt University
Nashville, Tennessee, 37235

L_2^m-stable digital-control networks for multiple continuous passive plants.

Nicholas Kottenstette and Nikhil Chopra

TECHNICAL REPORT

ISIS-09-103

A constructive method is presented in which L_2^m-stability can be guaranteed for networked control of multiple *passive* plants in spite random time varying delays and data dropouts. The passive plants are interfaced to a wave variable based *passive sampler* (PS) and *passive hold* (PH) which allows a passive digital control network to be constructed. A *power junction* is used to facilitate the interconnection of multiple passive plants and passive digital controllers. The power junction preserves passivity by guaranteeing that the overall power input to the system is greater than or equal to the power leaving the system. There are numerous ways to implement the power junction including the *averaging power junction* and the *consensus power junction* which are studied in this paper. In particular, a detailed steady state analysis is provided which relates the corresponding controller inputs to the plants outputs. The construction of our digital control network is completed by interconnecting the digital controllers to an *inner-product equivalent sampler* and zero-order hold (*IPESH*) which allows us to prove L_2^m-stability. Initial simulated results are also presented in which we compare performance using a *averaging power junction* and a *consensus power junction.*

1. INTRODUCTION

The primary goal of our research is to develop reliable wireless digital control networks Antsaklis and Baillieul (2004, 2007). In the past we have shown numerous results related to the control of a single continuous time *passive* plant with a single digital controller over a network. In particular we have shown how to create a *l_2^m-stable* digital control network for a continuous *passive* plant (Kottenstette and Antsaklis, 2007, Theorem 4) and built on this result to show that the controller can be run in an asynchronous manner (Kottenstette and Antsaklis, 2008b, Theorem 1). We have also shown how a continuous time stability result (*L_2^m-stability*) can be achieved with a *passive* digital controller by interfacing a continuous time *passive* plant to a passive sampler (PS) and passive hold (PH) (Kottenstette et al., 2008, Corollary 1). The key is to transmit control and sensor data in the form of *wave variables* over networks similar to those depicted in (Kottenstette and Antsaklis, 2007, Fig. 2). The use of *wave variables* allows the network controlled system to remain stable when subject to both fixed time delays and data dropouts. In addition, if duplicate wave variable transmissions are dropped, then the network will remain stable in spite of time varying delays. Recently we have shown how this framework can be modified to control multiple discrete-time passive plants over a wireless network by using a *power junction* and also guarantee l_2^m-stability (Kottenstette et al., 2009, Theorem 1). We noted in (Kottenstette et al., 2009, Section II-B) that L_2^m-stability results can also be shown with a power junction if continuous time plants were interfaced to a PS and PH. Figure 1 shows this proposed configuration which we provide a detailed analysis of. In doing so, we will introduce the *consensus power junction* which is based on a recent work related to passivity based synchronizing networks which use continuous time feedback Chopra and Spong (2006).

The main research challenge is to develop a formal way to *construct* a digital control network in which multiple continuous time plants and digital controllers can be interconnected such that the overall system remains stable and can change how the plants behave. This stability should be guaranteed in spite *random* time delays and data dropouts which are inherent to wireless networks. Furthermore we would like our statement on stability to have a *deterministic* and *continuous* time characteristic, specifically L_2^m stability. In regards to changing the plants behavior we would like to show that the plants can tolerate disturbances and track a desired set-point as quickly and as closely as possible. This paper shows how the *power junction* in conjunction with the passive sampler (PS) and passive hold (PH) can address this problem and guarantee L_2^m-stability. Furthermore it carefully derives the steady state responses of the plant outputs in regards to a set of steady state controller (and plant) inputs.

The *power junction* is an abstraction to interconnect wave variables from multiple controllers and plants such that the total power input is always greater than or equal to the total power output (Kottenstette et al., 2009, Definition 1). Interconnecting wave variables in a 'power preserving' manner has appeared in the telemanipulation literature to augment potential position drift by modifying one of the waves u_m in a *passive* manner (Niemeyer and Slotine, 2004, Fig. 9). Other abstractions to interconnect wave variables have also appeared in the wave digital filtering literature Fettweis (1986). Finally, a *consensus power junction* will be introduced which interconnects wave variables to plants in a similar manner as discussed in Chopra and Spong (2006) except: i) 'positive-feedback' loops are not allowed (which results from balanced graph interconnections, and we provide a motivating example to avoid such loops) ii) a controller can be explicitly used to steer the plants to a desired set-point and iii) the information does not need to be transmitted as a continuous-time waveform.

In this paper we show how the (*consensus* or *averaging*) and *power junction* in conjunction with a PS and PH makes it possible to allow m digital-controllers to control up to $n - m$ continuous-time-plants. We prove that such a network can be shown to be *L_2^m-stable* if all the interconnected plants and controllers are *strictly-output passive.* This paper differs is a significant refinement of our earlier work including Kottenstette and Antsaklis (2008a) in which the *power junction* first appeared and was significantly refined in Kottenstette et al. (2009) for the discrete time case. This paper, on the other hand, uses the PS and PH in conjunction with the power junction to construct a digital control system for multiple continuous time plants and controllers which can achieve L_2^m-stability. A complete steady-state analysis for the *averaging power junction* (Definition 2) is provided in this paper. We introduce the *consensus power junction* (Definition 3), show that it satisfies the conditions for the power junction (Lemma 4) and provide a steady state analysis (Theorem 17). A detailed set of simulations are presented in which two continuous

0

Contract/grant sponsor (number): NSF (NSF-CCF-0820088)
Contract/grant sponsor (number): DOD (N00164-07-C-8510)
Contract/grant sponsor (number): Air Force (FA9550-06-1-0312)
Award sponsor (name): University of Maryland (Minta Martin Research Award)

time plants are controlled over a digital network by digital-'PID' controller which are connected over a network using either an averaging power junction or consensus power junction.

The rest of the paper is organized as follows: i) Section 2 presents all that is required to design network control systems for multiple-continuous-plants interconnected to (multiple)-digital-controllers through the power junction (Section 2.2) and the PS and PH (Section 2.3) which are L_2^m stable (Section 2.4), a detailed steady-state response analysis (Section 2.5) , ii) Section 3 presents a detailed set of simulations in which two continuous time plants are controlled over a digital network by a digital-'PID' controller which are connected over a network using either an averaging power junction or consensus power junction, iii) Section 4 provides our conclusions and a more specific summary of our contributions, iv) Appendix A provides a review on passivity while Appendix B provides detailed proofs for the results presented in this paper.

2. NETWORKED CONTROL DESIGN

2.1 Wave Variables

Networks of a *passive* plant and controller are typically interconnected using *power variables*. *Power variables* are generally denoted with an *effort* and *flow* pair (e_*,f_*) whose product is power. They are typically used to show the exchange of energy between two systems using *bond graphs* Breedveld (2006); Golo et al. (2003). However, when these *power variables* are subject to communication delays the communication channel ceases to be *passive* which leads to network instabilities. Wave variables allow *effort* and *flow* variables to be transmitted over a network while remaining *passive* when subject to arbitrary fixed time delays and data dropouts Niemeyer and Slotine (2004).

$$u_{pk}(t) = \frac{1}{\sqrt{2b}}(bf_{pk}(t) + e_{dck}(t)),\ k \in \{m+1,\dots,n\} \quad (1)$$

$$v_{pk}(t) = \frac{1}{\sqrt{2b}}(bf_{pk}(t) - e_{dck}(t)) \quad (2)$$

$$v_{cj}(i) = \frac{1}{\sqrt{2b}}(bf_{dpj}(i) - e_{cj}(i)),\ j \in \{1,\dots,m\} \quad (3)$$

$$u_{cj}(i) = \frac{1}{\sqrt{2b}}(bf_{dpj}(i) + e_{dpj}(i)) \quad (4)$$

(1) can be thought of as each sensor output in a *wave variable* form for each plant $G_{pk},\ k \in \{m+1,\dots,n\}$ depicted in Fig. 1. Likewise, (3) can be thought of as each command output in a *wave variable* form for each controller $G_{cj},\ j \in \{1,\dots,m\}$ depicted in Fig. 1. The symbol $i \in \{0,1,\dots\}$ depicts discrete time for the controllers, and the symbol $t \in \mathbb{R}$ denotes continuous time and the two are related to the sample and hold time (T_s) such that $t = iT_s$. (1) and (2) respectively satisfy the following equality $\forall\ k \in \{m+1,\dots,n\}$:

$$\frac{1}{2}(u_{pk}^{\mathsf{T}}(t)u_{pk}(t) - v_{pk}^{\mathsf{T}}(t)v_{pk}(t)) = f_{pk}^{\mathsf{T}}(t)e_{dck}(t) \quad (5)$$

Similarly, (3) and (4) respectively satisfy the following equality $\forall\ j \in \{1,\dots,m\}$:

$$\frac{1}{2}(u_{cj}^{\mathsf{T}}(i)u_{cj}(i) - v_{cj}^{\mathsf{T}}(i)v_{cj}(i)) = f_{dpj}^{\mathsf{T}}(i)e_{cj}(i). \quad (6)$$

Denote $I \in \mathbb{R}^{m_s \times m_s}$ as the identity matrix. When implementing the wave variable transformation the continuous time plant "outputs" $(u_{pk}(t), e_{dck}(t))$ are related to the corresponding "inputs" $(v_{pk}(t), f_{pk}(t))$ as follows (Fig. 1):

$$\begin{bmatrix} u_{pk}(t) \\ e_{dck}(t) \end{bmatrix} = \begin{bmatrix} -I & \sqrt{2b}I \\ -\sqrt{2b}I & bI \end{bmatrix} \begin{bmatrix} v_{pk}(t) \\ f_{pk}(t) \end{bmatrix} \quad (7)$$

analogously (7) can be used to compute the continuous time controller "outputs" $(u_{rj}(t), e_{cj}(t))$ in terms of the controller "inputs" $(v_{rj}(t), r_{cj}(t))$. Next, the discrete time controller "outputs" $(v_{cj}(i), f_{dpj}(i))$ are related to the corresponding "inputs" $(u_{cj}(i), e_{cj}(i))$ as follows (Fig. 1):

$$\begin{bmatrix} v_{cj}(i) \\ f_{dpj}(i) \end{bmatrix} = \begin{bmatrix} I & -\sqrt{\frac{2}{b}}I \\ \sqrt{\frac{2}{b}}I & -\frac{1}{b}I \end{bmatrix} \begin{bmatrix} u_{cj}(i) \\ e_{cj}(i) \end{bmatrix} \quad (8)$$

analogously (8) can be used to compute the discrete time controller "outputs" $(v_{rj}(i), r_{cj}(i))$ in terms of the controller "inputs" $(u_{rj}(i), e_{cj}(i))$.

The *power junction* indicated in Fig. 1 by the symbol PJ has waves entering and leaving the power junction as indicated by the arrows. Waves leaving the controllers v_{cj} and entering the power junction v_j in which $j \in \{1,\dots,m\}$ have the following relationship

$$v_j(i) = v_{cj}(i - p_j(i))$$

in which $p_j(i)$ denotes the time varying delay in transmitting the control wave from 'controller-j' to the power junction. Next, the input wave to the plant v_{pk} is a delayed version of the outgoing wave from the *power junction* $v_k,\ k \in \{m+1,\dots,n\}$ such that

$$v_{pk}(i) = v_k(i - p_k(i)),\ k \in \{m+1,\dots,n\}$$

in which $p_k(i)$ denotes the discrete time varying delay in transmitting the outgoing wave to 'plant-k'. In Fig. 1 the delays are represented as fixed for the discrete time case (i.e. z^{-p_k}). Next, the outgoing wave from each plant u_{pk} is related to the wave entering the power junction $u_k,\ k \in \{m+1,\dots,n\}$ as follows:

$$u_k(i) = u_{pk}(i - c_k(i)),\ k \in \{m+1,\dots,n\}$$

in which $c_k(i)$ denotes the discrete time varying delay in transmitting the wave from 'plant-k' to the power junction. Last, the input wave to the controller u_{cj} is a delayed version of the outgoing wave from the *power junction* $u_j,\ j \in \{1,\dots,m\}$ such that

$$u_{cj}(i) = u_j(i - c_j(i)),\ j \in \{1,\dots,m\}$$

in which $c_j(i)$ denotes the discrete time varying delay in transmitting the wave from the power junction to 'controller-j'. In Fig. 1 the delays are represented as fixed for the discrete time case (i.e. z^{-c_j}).

2.2 The Power Junction

The "power junction" depicted in Fig. 1 provides a general way to interconnect multiple plants to multiple controllers, and we shall see that it can be implemented in numerous ways.

Definition 1. Kottenstette et al. (2009)[Definition 1] A "power junction" is implemented as follows (see Fig. 1): n systems are interconnected to a power junction using the corresponding wave variable pairs (u_1, v_1), (u_2, v_2), ...,

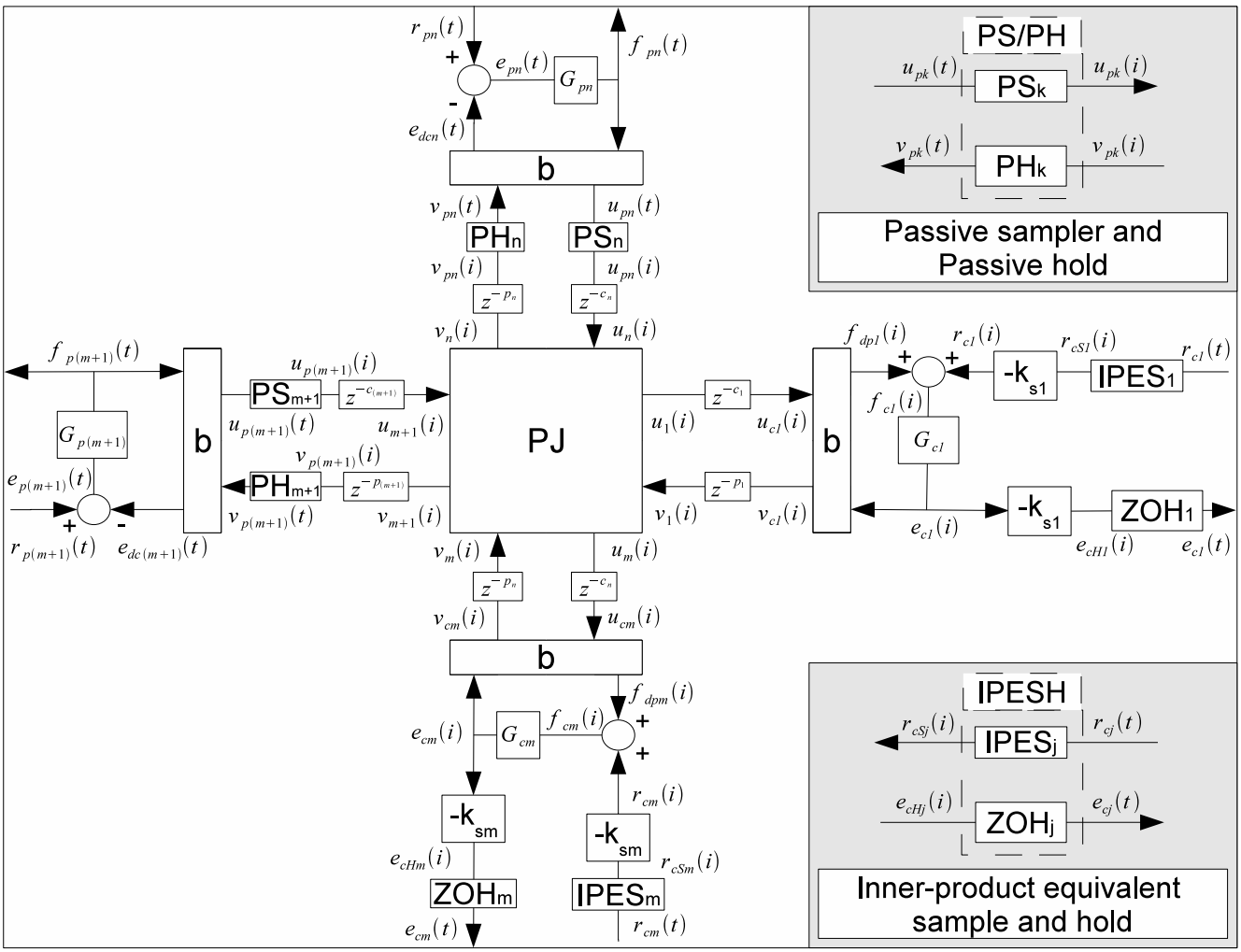

Fig. 1. An L_2^m-stable *power junction* control network.

(u_n, v_n). The *power-output* pairs $(u_j, v_j),\ j \in \{1, \ldots, m\}$ (in which $u_j \in \mathbb{R}^{m_s}$ is an outgoing wave and $v_j \in \mathbb{R}^{m_s}$ is an incoming wave to the power junction) are related to the *power-input* pairs $(u_k, v_k),\ k \in \{m+1, \ldots, n\}$ (in which $u_k \in \mathbb{R}^{m_s}$ is an incoming wave and $v_k \in \mathbb{R}^{m_s}$ is an outgoing wave from the power junction) such that

$$\sum_{k=m+1}^{n} (u_k^{\mathsf{T}} u_k - v_k^{\mathsf{T}} v_k) \geq \sum_{j=1}^{m} (u_j^{\mathsf{T}} u_j - v_j^{\mathsf{T}} v_j) \qquad (9)$$

holds. In other words the total *power-input* is always greater than or equal to the total *power-output* from the power junction. When (9) is satisfied by an equality, the power junction is not only *passive* but *lossless*.

The *averaging power junction* is one implementation we will analyze which satisfies Definition 1 (Kottenstette et al. (2009)[Lemma 2]). We add a minor modification to the averaging power junction definition presented in Kottenstette et al. (2009)[Definition 2] which improves overall system performance while still satisfying Definition 1.

Definition 2. n systems are interconnected to an *averaging power junction* using the corresponding wave variable pairs (u_1, v_1), (u_2, v_2), $\ldots$, (u_n, v_n). The *power-output* pairs are denoted $(u_j, v_j),\ j \in \{1, \ldots, m\}$ in which $u_j \in \mathbb{R}^{m_s}$ is an outgoing wave and $v_j \in \mathbb{R}^{m_s}$ is an incoming wave to the averaging power junction. The *power-input* pairs are denoted $(u_k, v_k),\ k \in \{m+1, \ldots, n\}$ in which $u_k \in \mathbb{R}^{m_s}$ is an incoming wave and $v_k \in \mathbb{R}^{m_s}$ is an outgoing wave from the averaging power junction. Each l^{th} component ($l \in \{1, \ldots, m_s\}$) of the outgoing waves v_k (denoted v_{k_l}) are computed from the respective l^{th} component of the incoming waves v_j (denoted v_{j_l}) as follows:

$$\begin{aligned}
\mathsf{sf}_v &= \frac{|\sum_{j=1}^{m} v_{j_l}|}{\sum_{j=1}^{m} |v_{j_l}|} \\
v_{k_l} &= \mathsf{sf}_v \mathsf{sgn}(\sum_{j=1}^{m} v_{j_l}) \frac{\sqrt{\sum_{j=1}^{m} v_{j_l}^2}}{\sqrt{n-m}},\ k \in \{m+1, \ldots, n\} \\
&= \frac{v_{1_l}}{\sqrt{n-1}} \text{ when } m = 1
\end{aligned}$$

Similarly, each l^{th} component ($l \in \{1, \ldots, m_s\}$) of the outgoing waves u_j (denoted u_{j_l}) are computed from the respective l^{th} component of the incoming waves u_k (denoted u_{k_l}) as follows:

$$\mathsf{sf}_u = \frac{|\sum_{k=m+1}^{n} u_{k_l}|}{\sum_{k=1+1}^{n} |u_{k_l}|}$$

$$u_{j_l} = \mathsf{sf}_u \mathtt{sgn}(\sum_{k=m+1}^{n} u_{k_l}) \frac{\sqrt{\sum_{k=m+1}^{n} u_{k_l}^2}}{\sqrt{m}},\ j \in \{1,\ldots,m\}$$
$$= \mathsf{sf}_u \mathtt{sgn}(\sum_{k=2}^{n} u_{k_l}) \sqrt{\sum_{k=2}^{n} u_{k_l}^2} \text{ when } m = 1.$$

In addition to evaluating the averaging power junction, we introduce the *consensus power junction*.

Definition 3. n systems are interconnected to a *consensus power junction* using the corresponding wave variable pairs (u_1, v_1), (u_2, v_2), $\ldots$, (u_n, v_n). The *power-output* pairs are denoted $(u_j, v_j),\ j \in \{1,\ldots,m\}$ in which $u_j \in \mathbb{R}^{m_s}$ is an outgoing wave and $v_j \in \mathbb{R}^{m_s}$ is an incoming wave to the consensus power junction. The *power-input* pairs are denoted $(u_k, v_k),\ k \in \{m+1,\ldots,n\}$ in which $u_k \in \mathbb{R}^{m_s}$ is an incoming wave and $v_k \in \mathbb{R}^{m_s}$ is an outgoing wave from the consensus power junction. The incoming wave from plant n denoted $u_n(i)$ is related to the outgoing wave to controller 1 denoted $u_1(i)$ such that

$$u_1(i) = u_n(i). \tag{10}$$

If $m > 1$ then the incoming wave $v_j(i)$ is related to the outgoing wave $u_{j+1}(i)$ to the next controller such that

$$u_{j+1}(i) = v_j(i)\ j \in \{1,\ldots,m-1\}. \tag{11}$$

Next, the final output from the m^{th} controller is connected to the first plant such that

$$v_{m+1}(i) = v_m(i). \tag{12}$$

If $n > m+1$ then the incoming wave $u_k(i)$ is related to the outgoing wave $v_{k+1}(i)$ such that

$$v_{k+1}(i) = u_k(i)\ k \in \{m+1,\ldots,n-1\}. \tag{13}$$

Lemma 4. The consensus power junction (Definition 3) satisfies the inequality in (9) in order to be a "power junction" (Definition 1), furthermore it satisfies (9) as an equality and is therefore *lossless*.

The proof of Lemma 4 is in Appendix B.1.

2.3 Passive Sampling and Holding.

In Kottenstette et al. (2008) it was shown how a passive sampler (PS) a passive hold (PH) in conjunction with a *inner-product equivalent sampler* (*IPES*) and zero-order-hold (*ZOH*) can be used to achieve a L_2^m-stable system consisting of a passive robot and a digital controller. As can be seen in Fig. 1 we have connected the PS and PH to each plant, while connecting the (*IPES*) and zero-order-hold (*ZOH*) block to each digital controller in order to relate $r_{cj}(i)$ to $r_{cj}(t)$ and $e_{cj}(i)$ to $e_{cj}(t)$ in a passivity preserving manner. Therefore we recall the following set of definitions:

Definition 5. The passive samplers denoted (PS_k) and the corresponding passive holds denoted (PH_k) $\forall k \in \{m+1,\ldots,n\}$ must be implemented such that the following inequality is satisfied $\forall N > 0$:

$$\int_0^{NT_s} (u_{pk}^{\mathsf{T}}(t)u_{pk}(t) - v_{pk}^{\mathsf{T}}(t)v_{pk}(t))dt - \sum_{i=0}^{N-1} (u_{pk}^{\mathsf{T}}(i)u_{pk}(i) - v_{pk}^{\mathsf{T}}(i)v_{pk}(i)) \geq 0. \tag{14}$$

This condition ensures that no energy is generated by the sample and hold devices, and thus, passivity is preserved. One way to implement the PS and PH is to use the *averaging passive sampler and hold*.

Definition 6. The *averaging passive samplers* denoted (PS_k) and the corresponding *averaging passive holds* denoted (PH_k) $\forall k \in \{m+1,\ldots,n\}$ is implemented such that for each l^{th} component ($l \in \{1,\ldots,m_s\}$) of the discrete-time-sampled waves $u_{pk}(i) \in \mathbb{R}^{m_s}$ (denoted $u_{pk_l}(i)$) is determined from the respective l^{th} component of the continuous-time wave $u_{pk}(t) \in \mathbb{R}^{m_s}$ (denoted $u_{pk_l}(t)$) using PS_k as follows:

$$u_{pk_l}(i) = \sqrt{\int_{(i-1)T_s}^{iT_s} u_{pk_l}^2(t)dt}\ \mathtt{sgn}(\int_{(i-1)T_s}^{iT_s} u_{pk_l}(t)dt) \tag{15}$$

and the continuous-time wave $v_{pk}(t) \in \mathbb{R}^{m_s}$ is determined from the discrete-time waves $v_{pk}(i) \in \mathbb{R}^{m_s}$ in terms of each of their respective l^{th} components using PH_k as follows:

$$v_{pk_l}(t) = \frac{1}{\sqrt{T_s}} v_{pk_l}(i),\ t \in [iT_s, (i+1)T_s). \tag{16}$$

Using a PS and PH such as the *averaging passive sampler and hold* we can now relate continuous time variables to discrete time wave variables associated with each plant G_{pk}, $k \in \{m+1,\ldots,n\}$. Substituting (5) into (14) results in the following inequality for each plant

$$\int_0^{NT_s} f_{pk}^{\mathsf{T}}(t)e_{dck}(t) \geq \sum_{i=0}^{N-1} (u_{pk}^{\mathsf{T}}(i)u_{pk}(i) - v_{pk}^{\mathsf{T}}(i)v_{pk}(i)). \tag{17}$$

Next, we would like to determine how (17) relates to the corresponding pair of waves entering and leaving the *power junction* $(u_k(i), v_k(i))$. In order to do so, we state the following proposition which summarizes observations made in Berestesky et al. (2004); Stramigioli et al. (2005); Kottenstette and Antsaklis (2007, 2008b).

Proposition 7. More generally, given two pairs of waves $(u(i), v_d(i))$, $(u_d(i), v(i))$ in which the received-waves with the d-subscript are related to their corresponding non-delayed transmitted-counterparts such that

$$u_d(i) = \begin{cases} u(i - d_u(i)), & \text{if } d_u(i) \leq i \\ 0, & \text{otherwise.} \end{cases}$$

$$v_d(i) = \begin{cases} v(i - d_v(i)), & \text{if } d_v(i) \leq i \\ 0, & \text{otherwise.} \end{cases}$$

where $d_u(i),\ d_v(i) \in \{1, 2, \ldots,\}$ is the respective delay at time i. A necessary condition for

$$\sum_{i=0}^{N-1} u^{\mathsf{T}}(i)u(i) - v_d^{\mathsf{T}}(i)v_d(i) \geq \sum_{i=0}^{N-1} u_d^{\mathsf{T}}(i)u_d(i) - v^{\mathsf{T}}(i)v(i) \tag{18}$$

or equivalently

$$\sum_{i=0}^{N-1} u^{\mathsf{T}}(i)u(i) - u_d^{\mathsf{T}}(i)u_d(i) + \sum_{i=0}^{N-1} v^{\mathsf{T}}(i)v(i) - v_d^{\mathsf{T}}(i)v_d(i) \geq 0$$

to be satisfied for all $N > 0$ is that both

$$\sum_{i=0}^{N-1} u^{\mathsf{T}}(i)u(i) - u^{\mathsf{T}}(i-d_u(i))u(i-d_u(i)) \geq 0 \text{ and}$$
$$\sum_{i=0}^{N-1} v^{\mathsf{T}}(i)v(i) - v^{\mathsf{T}}(i-d_v(i))v(i-d_v(i)) \geq 0$$

are satisfied for all $N > 0$. Therefore:

I. if delays are fixed ($d_u(i) = d_u, d_v(i) = d_v$) then (18) is always satisfied,
II. if the delays are such that data is always dropped ($d_u(i) = d_v(i) = (i+1)$) then (18) is always satisfied,
III. if the delays are switched arbitrarily between a constant delay or a drop-out delay ($d_u(i) \in \{d_u, (i+1)\}$ and $(d_v(i) \in \{(i+1), d_v\})$) then (18) is always satisfied,
IV. if the delays are such that no duplicate wave-transmissions are processed then (18) is always satisfied, more precisely if we denote the set of received indexes up to time $N-1$ for u_d and v_d as $\mathcal{D}_u = \{0 - d_u(0), 1 - d_u(1), \ldots, (N-1) - d_u(N-1)\}$ and $\mathcal{D}_v = \{0 - d_v(0), 1 - d_v(1), \ldots, (N-1) - d_v(N-1)\}$ respectively and
   - each index $i \in \{0, 1, \ldots, N-1\}$ appears in $\mathcal{D}_u$ no more than once and
   - each index $i \in \{0, 1, \ldots, N-1\}$ appears in $\mathcal{D}_v$ no more than once.

   An example of a delay which violates this final condition is when $d_u(i) = i$ in which $\mathcal{D}_u = \{0, 0, \ldots, 0\}$ and the index 0 appears N times.

TCP/IP is a transmission protocol which will satisfy (18) however the UDP protocol could replicate packets and violate (18). Applications which choose to use UDP can be easily modified to satisfy Propositions 7-IV.

We can now state the following corollary which relates (17) to the corresponding pair of waves entering and leaving the *power junction* $(u_k(i), v_k(i))$.

Corollary 8. All $n-m$ continuous time plant (flows $f_{pk}(t)$ and effort $e_{dck}(t)$) pairs depicted in Fig. 1 are related to their respective pair of waves entering and leaving the *power junction* $(u_k(i), v_k(i))$ such that $\forall k \in \{m+1, \ldots, n\}$

$$\int_0^{NT_s} f_{pk}^{\mathsf{T}}(t)e_{dck}(t) \geq \sum_{i=0}^{N-1}(u_k^{\mathsf{T}}(i)u_k(i) - v_k^{\mathsf{T}}(i)v_k(i))$$
$$\langle f_{pk}(t), e_{dck}(t)\rangle_{NT_s} \geq \|(u_k(i))_N\|_2^2 - \|(v_k(i))_N\|_2^2$$
$$\langle f_{pk}, e_{dck}\rangle_{NT_s} \geq \|(u_k)_N\|_2^2 - \|(v_k)_N\|_2^2 \quad (19)$$

is satisfied if the wave variable communication time-delays $c_k(i) = d_u(i)$, $p_k(i) = d_v(i)$ satisfy any of the conditions listed in Proposition 7.

See Appendix A for an explanation of the short hand notation used in (19), since T_s is typically not an integer, we will typically drop the i or t symbol and use N to refer to extended discrete-time l_2^m norms and NT_s to refer to extended L_2^m norms. In an analogous manner we can relate the control effort and flow variables $(e_{cj}(i), f_{dpj}(i))$ to the power junction wave variables $(u_j(i), v_j(i)\ \forall j \in \{1, \ldots, m\}$ for the m-digital controllers.

Corollary 9. All m discrete time controller (flows $f_{dpj}(i)$ and efforts $e_{cj}(i)$) pairs depicted in Fig. 1 are related to their respective pair of waves leaving and entering the *power junction* $(u_j(i), v_j(i))$ such that $\forall j \in \{1, \ldots, m\}$

$$\|(u_j)_N\|_2^2 - \|(v_j)_N\|_2^2 \geq \|(u_{cj})_N\|_2^2 - \|(v_{cj})_N\|_2^2$$
$$\|(u_j)_N\|_2^2 - \|(v_j)_N\|_2^2 \geq \langle e_{cj}, f_{dpj}\rangle_N \quad (20)$$

is satisfied if the wave variable communication time-delays $c_j(i) = d_u(i)$, $p_j(i) = d_v(i)$ satisfy any of the conditions listed in Proposition 7.

Which leads us to the following lemma.

Lemma 10. The m discrete time controller (flows $f_{dpj}(i)$ and efforts $e_{cj}(i)$) pairs $j \in \{1, \ldots, m\}$ are related to the $n-m$ continuous time plant (flows $f_{pk}(t)$ and effort $e_{dck}(t)$) pairs $k \in \{m+1, \ldots, n\}$ depicted in Fig. 1 as follows

$$\sum_{k=m+1}^{n} \langle f_{pk}(t), e_{dck}\rangle_{NT_s} \geq \sum_{j=1}^{m} \langle e_{cj}(i), f_{dpj}(i)\rangle_N \quad (21)$$

if the wave variable communication time-delays $c_j(i) = c_k(i) = d_u(i)$, $p_j(i) = p_k(i) = d_v(i)$ satisfy any of the conditions listed in Proposition 7.

The proof of Lemma 10 is in Appendix B.2.

In order to show L_2^m stability of our digital control network depicted in Fig. 1 we need to relate $\forall j \in \{1, \ldots, m\}$ the discrete-time reference and effort variables associated with each digital controller G_{cj} (denoted by the respective tuple $(r_{cj}(i), e_{cj}(i))$) to a continuous-time reference and effort variable counterpart which we denote by the respective tuple $(r_{cj}(t), e_{cj}(t))$. In order to make this comparison we used the *inner-product equivalent sampler* (denoted IPES_j in Fig. 1) and a zero-order-hold (denoted ZOH_j in Fig. 1). We will refer to the pair of these devices as the *inner-product equivalent sample and hold* (*IPESH*). The *IPESH* was formally defined in (Kottenstette and Antsaklis, 2007, Definition 4) in order to relate a continuous time plant to a discrete time counterpart. The continuous time plant was preceded by a *ZOH* at its input and its output was proceeded by an *IPES*. In Kottenstette et al. (2008) however we 'switched' the ordering in which the *IPES* precedes the input to a discrete time plant and the *ZOH* proceeds the output of the discrete time plant.

Definition 11. The *m-inner-product equivalent sample and hold*'s depicted in Fig. 1 by the pair of respective symbols (IPES_j,ZOH_j) $j \in \{1, \ldots, m\}$ in which the inputs are denoted by the pair $(r_{cj}(t), e_{cHj}(i))$ and the outputs are denoted by the pair $(r_{cSj}(i), e_{cj}(t))$. The *inner-product equivalent sampler* (*IPES*) is implemented by sampling $r_{cj}(t)$ at a rate (T_s) such that $\forall N > 0$:

$$x(t) = \int_0^t r_{cj}(\tau)d\tau$$
$$r_{cSj}(i) = x((i+1)T_s) - x(iT_s). \quad (22)$$

The *ZOH* is implemented as follows:

$$e_{cj}(t) = e_{cHj}(i),\ t \in [iT_s, (i+1)T_s) \quad (23)$$

Corollary 12. Using the *IPESH* as stated in Definition 11 we have that

$$\int_0^{NT_s} e_{cj}^{\mathsf{T}}(t) r_{cj}(t) dt = \sum_{i=0}^{N-1} \int_{iT_s}^{(i+1)T_s} e_{cj}^{\mathsf{T}}(t) r_{cj}(t) dt$$

in which substituting (23) for the *ZOH* results in

$$\langle e_{cj}, r_{cj} \rangle_{NT_s} = \sum_{i=0}^{N-1} e_{cHj}^{\mathsf{T}}(i) \int_{iT_s}^{(i+1)T_s} r_{cj}(t) dt$$

and finally substituting (22) for the *IPES* results in

$$\langle e_{cj}, r_{cj} \rangle_{NT_s} = \sum_{i=0}^{N-1} e_{cHj}^{\mathsf{T}}(i) r_{cSj}(i)$$

$$\langle e_{cj}, r_{cj} \rangle_{NT_s} = \langle e_{cHj}, r_{cSj} \rangle_N \text{ holds.} \tag{24}$$

Using the *ZOH* as stated in Definition 11 we also have the property that

$$\int_0^{NT_s} e_{cj}^{\mathsf{T}}(t) e_{cj}(t) dt = \sum_{i=0}^{N-1} \int_{iT_s}^{(i+1)T_s} e_{cj}^{\mathsf{T}}(t) e_{cj}(t) dt$$

$$\|(e_{cj})_{NT_s}\|_2^2 = T_s \|(e_{cHj})_N\|_2^2 \text{ holds.} \tag{25}$$

Finally Fig. 1 possesses some scalar scaling gains $k_s \in \mathbf{R}^+$ to account for the using the power-junction, PS and PH and the *IPESH*, such that for all $j \in \{1, \ldots, m\}$:

$$r_{cj}(i) = -k_{sj} r_{cSj}(i) \tag{26}$$

$$e_{cj}(i) = -\frac{1}{k_{sj}} e_{cHj}(i). \tag{27}$$

Using Corollary 12, (26), and (27) we have the following relationships

$$\begin{aligned} \langle e_{cj}, r_{cj} \rangle_N &= \langle e_{cHj}, r_{cSj} \rangle_N \\ \langle e_{cj}, r_{cj} \rangle_N &= \langle e_{cj}, r_{cj} \rangle_{NT_s} \end{aligned} \tag{28}$$

$$\begin{aligned} \|(e_{cj})_N\|_2^2 &= \frac{1}{k_{sj}^2} \|(e_{cHj})_N\|_2^2 \\ \|(e_{cj})_N\|_2^2 &= \frac{1}{T_s k_{sj}^2} \|(e_{cj})_{NT_s}\|_2^2. \end{aligned} \tag{29}$$

2.4 L_2^m Stable Power Junction Networks

Fig. 1 depicts m controllers interconnected to $n-m$ plants using a *power junction*. It can be shown that this network will remain L_2^m*-stable* when subject to either fixed delays and/or data dropouts. Furthermore we can show how to safely handle time varying delays by dropping duplicate transmissions from the *power junction*. Please refer to Appendix A for corresponding definitions or nomenclature.

Theorem 13. For the network controlled system depicted in Fig. 1, assume all the wave variable communication time-delays $c_j(i) = c_k(i) = d_u(i)$, $p_j(i) = p_k(i) = d_v(i)$ satisfy any one of the conditions listed in Proposition 7. Then the system is:

I. L_2^m*-stable* if all plants $G_{pk}(e_{pk}(t))$, $k \in \{m+1, \ldots, n\}$ and all controllers $G_{cj}(f_{cj}(i)), j \in \{1, \ldots, m\}$ are *strictly-output passive*.
II. *passive* if all plants $G_{pk}(e_{pk}(t))$, $k \in \{m+1, \ldots, n\}$ and all controllers $G_{cj}(f_{cj}(i)), j \in \{1, \ldots, m\}$ are *passive*.

The proof of Theorem 13 is in Appendix B.3.

2.5 Steady State Response of Networked Control System

It is desired to relate the controller reference inputs $\{r_{c1}(t), \ldots, r_{cm}(t)\}$ and plant disturbance inputs $\{r_{p(m+1)}(t), \ldots, r_{pn}(t)\}$ to the corresponding controller efforts $\{e_{c1}(t), \ldots, e_{cm}(t)\}$ and plant flows $\{f_{p(m+1)}(t), \ldots, f_{pn}(t)\}$. Since our stability results apply to both linear and nonlinear systems we will focus our initial analysis to the steady-state case $\lim_{t\to\infty} f_{p(m+1)}(t)$. In particular, we determine the steady-state system responses when using either the averaging power junction or the consensus power junction under the following assumptions.

Assumption 14. Each plant, denoted $G_{pk} : e_{pk}(t) \to f_{pk}(t)$ $k \in \{m+1, \ldots, n\}$, is a single-input-single-output (SISO) system with a steady-state gain denoted k_{pk} such-that

$$f_{pk}(0) = 0$$

$$e_{pk}(t) = \begin{cases} 0, & t < 0 \\ e_{pk}, & t \geq 0 \end{cases}$$

$$k_{pk} = \lim_{t\to\infty} \frac{f_{pk}(t)}{e_{pk}(t)}.$$

In a similar manner each controller, denoted $G_{cj} : f_{cj}(i) \to e_{cj}(i)$ $j \in \{1, \ldots, m\}$, is a SISO system with a steady-state gain denoted k_{cj} such-that

$$e_{cj}(0) = 0$$

$$f_{cj}(i) = \begin{cases} 0, & i < 0 \\ f_{cj}, & i \geq 0 \end{cases}$$

$$k_{cj} = \lim_{i\to\infty} \frac{e_{cj}(i)}{f_{cj}(i)}.$$

Furthermore, for simplicity, all wave variable communication time-delays $c_k(i) = d_u(i) = 1$, $p_k(i) = d_v(i) = 1$. To aid with the steady-state analysis we assume for the PS/PH blocks that

$$u_{pk}(i) = \sqrt{T_s} u_{pk}(iT_s) \text{ and} \tag{30}$$

$$v_{pk}(iT_s) = \frac{v_{pk}(i)}{\sqrt{T_s}}. \tag{31}$$

In addition we assume for the *IPESH* blocks that

$$r_{cSj}(i) = T_s r_{cj}(iT_s) \text{ such that}$$

$$r_{cj}(i) = -k_{sj} T_s r_{cj}(iT_s) \text{ and} \tag{32}$$

$$e_{cj}(iT_s) = e_{cHj}(i) = -k_{sj} e_{cj}(i). \tag{33}$$

Lemma 15. Under the assumptions listed in Assumption 14, the following equations hold for the plants interconnected by the power junction control network depicted in Fig. 1:

$$u_{pk}(i) = \frac{bk_{pk} - 1}{bk_{pk} + 1} v_{pk}(i) + \frac{\sqrt{T_s 2b} k_{pk}}{bk_{pk} + 1} r_{pk}(iT_s) \tag{34}$$

$$f_{pk}(iT_s) = \frac{\sqrt{2b} k_{pk}}{\sqrt{T_s}(bk_{pk} + 1)} v_{pk}(i) + \frac{k_{pk}}{bk_{pk} + 1} r_{pk}(iT_s). \tag{35}$$

The proof of Lemma 15 is in Appendix B.4.

Lemma 16. Under the assumptions listed in Assumption 14, the following equations hold for the controllers inter-connected by the power junction control network depicted in Fig. 1:

$$v_{cj}(i) = \frac{-k_{cj}+b}{k_{cj}+b}u_{cj}(i) + \frac{\sqrt{2b}T_s k_{cj}k_{sj}}{k_{cj}+b}r_{cj}(iT_s) \quad (36)$$

$$e_{cj}(iT_s) = -\frac{\sqrt{2b}k_{cj}k_{sj}}{k_{cj}+b}u_{cj}(i) + \frac{T_s b k_{cj}k_{sj}^2}{k_{cj}+b}r_{cj}(iT_s). \quad (37)$$

The proof of Lemma 16 is in Appendix B.5.

Theorem 17. Under the assumptions listed in Assumption 14, the following state equations can be used to determine the steady state response of the power junction control network depicted in Fig. 1 when using the averaging power junction:

$$u_k(i) = \frac{bk_{pk}-1}{bk_{pk}+1}v_{m+1}(i-2) + \frac{\sqrt{T_s 2b}k_{pk}}{bk_{pk}+1}r_{pk}$$

$$v_j(i) = \frac{-k_{cj}+b}{k_{cj}+b}u_1(i-2) + \frac{\sqrt{2b}T_s k_{cj}k_{sj}}{k_{cj}+b}r_{cj}$$

$$u_1(i-1) = \mathsf{sf}_u \mathtt{sgn}\Big(\sum_{k=m+1}^{n} u_k(i-1)\Big)\frac{\sqrt{\sum_{k=m+1}^{n} u_k^2(i-1)}}{\sqrt{m}}$$

$$v_{m+1}(i-1) = \mathsf{sf}_v \mathtt{sgn}\Big(\sum_{j=1}^{m} v_j(i-1)\Big)\frac{\sqrt{\sum_{j=1}^{m} v_j^2(i-1)}}{\sqrt{n-m}}.$$

Likewise the steady-state outputs $f_{pk}(iT_s)$ $e_{cj}(iT_s)$ are computed by substituting $v_{pk} = v_{m+1}(i-1)$ into (35) and substituting $u_{cj} = u_1(i-1)$ into (37) respectively.

It is a straight forward exercise for the reader to apply Lemma 15, Lemma 16, Definition 2, and Assumption 14 to verify Theorem 17. For the case of the consensus junction, a closed form solution can be found as stated in Theorem 18.

Theorem 18. Consider the case of a single controller and $n-1$ plants. Under the assumptions listed in Assumption 14, using (34), (35), (36) and (37), employing the consensus power junction, the following steady state equations hold:

$$\begin{aligned} u_{pk}(i) = &\left(\prod_{l=2}^{k}\alpha_l\right)\beta_1 u_{c1}(i) + \left(\prod_{l=2}^{k}\alpha_l\right)\beta_2 r_{c1}(iT_s) \\ &+ \sum_{l=2}^{k}\left(\prod_{s=l}^{k}\gamma_s\right) r_{pl}(iT_s) \end{aligned} \quad (38)$$

where $\alpha_k = \frac{bk_{pk}-1}{bk_{pk}+1}$, $\gamma_k = \frac{\sqrt{T_s 2b}k_{pk}}{bk_{pk}+1}$, $\beta_1 = \frac{-k_{c1}+b}{k_{c1}+b}$ and $\beta_2 = \frac{\sqrt{2b}T_s k_{c1}k_{s1}}{k_{c1}+b}$ and

$$u_{c1}(i) = \frac{\left(\prod_{k=2}^{n}\alpha_k\right)\beta_2 r_{c1}(iT_s) + \sum_{k=2}^{n}\left(\prod_{s=k}^{n}\gamma_s\right) r_{pk}(iT_s)}{1-\left(\prod_{k=2}^{n}\alpha_k\right)\beta_1} \quad (39)$$

The corresponding outputs $f_{pk}(iT_s)$ can be obtained by additionally using (35).

Furthermore, for the special case of a Proportional-Integral (PI) controller, if $bk_{pk} >> 1$, $k_{s1} = \frac{1}{\sqrt{T_s}}$, and all disturbances are zero, then $f_{pk}(iT_s) = r_{c1}(iT_s) \ \ \forall k$.

The proof of Theorem 18 is in Appendix B.6.

3. SIMULATIONS

In this section we present results from a detailed simulation in which a 'PID'-digital controller is used to control two continuous-time 'perturbed' linear-time-invariant (LTI) plants. We will compare performance of the overall system when the averaging power junction is used to when the consensus power junction. The digital controller will be synthesized using the *inner-product equivalent sample and hold-transform* as defined.

Definition 19. (Kottenstette et al., 2009, Definition 4) Let $H_p(s)$ and $H_p(z)$ denote the respective continuous and discrete time transfer functions which describe a passive plant. Furthermore, let T_s denote the respective sample and hold time. Finally, denote $\mathcal{Z}\{F(s)\}$ as the z-transform of the sampled time series whose Laplace transform is the expression of $F(s)$, given on the same line in (Franklin et al., 2006, Table 8.1 p.600). $H_p(z)$ is generated using the following *IPESH-transform*

$$H_p(z) = \frac{(z-1)^2}{T_s z}\mathcal{Z}\left\{\frac{H_p(s)}{s^2}\right\}.$$

Each plant to be simulated is described by the corresponding Laplace transform

$$G_{pk}(s) = \frac{k_{pk}}{s+\omega_{pk}}.$$

An 'integral' digital-controller with z-transform $G_{\mathsf{I}}(z)$ is synthesized by applying the *IPESH-transform* to the continuous time 'integral' controller model which is described by the corresponding Laplace transform

$$G_{\mathsf{I}}(s) = \frac{k_{\mathsf{I}}}{s+\epsilon k_{\mathsf{I}}}.$$

Note that $\epsilon > 0$ can be an arbitrarily small constant which is used to make the 'integral'-controller strictly-output passive. Next a 'derivative' digital-controller with z-transform $G_{\mathsf{D}}(z)$ is synthesized by applying the (*IPESH-transform*) to the continuous time (strictly-output passive) 'lead'-controller model which is described by the corresponding Laplace transform

$$G_{\mathsf{D}}(s) = k_{\mathsf{D}}\frac{\frac{NT_s}{\pi}s+1}{\frac{T_s}{\pi}s+1}.$$

Note that $N > 1$, is typically chosen to be around 10. We used the following nominal plant model to pick our 'PID' control parameters.

$$G_p(s) = \frac{k_p}{s+\omega_p}$$

$$k_p = \min_{k\in\{m+1,\ldots,n\}}\left(\frac{k_{pk}}{\omega_{pk}}\right)$$

$$\omega_p = \min_{k\in\{m+1,\ldots,n\}}(\omega_{pk})$$

The overall controller which will be evaluated will be of the following form

$$G_{\mathsf{PID}}(z) = k_{\mathsf{P}} + G_{\mathsf{I}}(z) + G_{\mathsf{D}}(z)$$

With our nominal plant given, we use the following loop-shaping formulas to select the control gains in terms of the nyquist frequency $\omega_{\mathsf{nyquist}} = \frac{\pi}{T_s}$.

$$k_{\mathsf{P}} = \alpha\frac{1}{3}\frac{\omega_{\mathsf{nyquist}}+\omega_p}{k_p}$$

$$k_{\mathsf{I}} = \alpha\frac{1}{3}\frac{\omega_{\mathsf{nyquist}}(\omega_{\mathsf{nyquist}}+\omega_p)}{k_p}$$

$$k_{\mathsf{D}} = \alpha\frac{1}{3}\frac{2}{1+N}\frac{\omega_{\mathsf{nyquist}}+\omega_p}{k_p}.$$

Table 1 summarizes all relevant simulation parameters.

Table 1. PJ simulation parameters.

Plant	Assumptions
G_{p2}	$k_{p2} = \{1, 1, 5\}$, $\omega_{p2} = \{1, 1, 1\}$
G_{p3}	$k_{p3} = \{1, 5, 1\}$, $\omega_{p3} = \{1, 5, 1\}$
G_p	$k_p = 1$, $\omega_p = 1$
k_s	$\frac{\sqrt{n-m}}{\sqrt{T_s m}} = \frac{\sqrt{2}}{\sqrt{T_s}}$ (averaging PJ)
k_s	$\frac{1}{\sqrt{T_s}}$(consensus PJ)
delays	$p_1 = c_1 = 4,\ c_2 = p_3 = 5,\ c_3 = p_2 = 6$
misc.	$\alpha = 1,\ N = 10,\ b = \{1, 2, 10\},\ T_s = .1$ seconds.

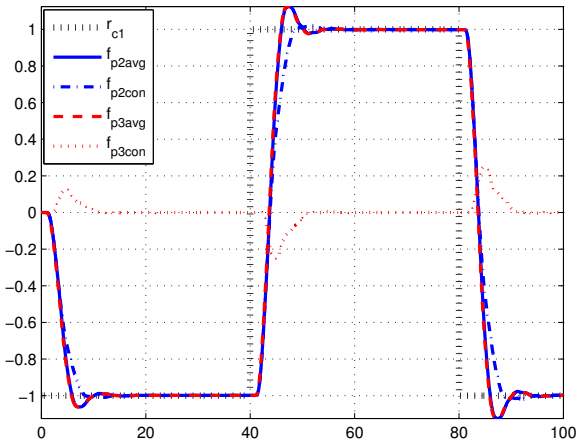

Fig. 2. Nominal velocity response $b = 1$, $i_p = 1$.

3.1 Nominal Step Response (no disturbances)

For the nominal case we assume that no disturbances are present and $r_{pk} = 0$. The reference, which will be the same for all simulations, to the controller consists of a square wave of the following form

$$r_{c1}(t) = -\mathtt{sgn}(\sin 2\pi.0125t).$$

We denote the plants simulated in our captions by using the plant index $i_p = \{1, 2, 3\}$. Using Table 1 as the key, a plant index $i_p = 2$ corresponds to $k_{p2} = 1$, $\omega_{p2} = 1$ and $k_{p3} = 5$, $\omega_{p3} = 5$ respectively in which each plant has the same steady-state gain but different dynamics. An index $i_p = 1$ is the base-line case in which both plants are identical $k_{p2} = k_{p3} = \omega_{p2} = \omega_{p3} = 1$. While an index $i_p = 3$ is the most difficult plant combination to achieve tracking since the steady-state gain is different ($k_{p2} = 5$, $\omega_{p2} = 1$, $k_{p3} = 1$, $\omega_{p3} = 1$). The velocity response is indicated in the legend in which f_{pkavg} denotes the velocity for each plant when using the averaging power junction and f_{pkcon} denotes the velocity for each plant when using the consensus power junction. Fig. 2 indicates that the averaging power junction achieves consensus $f_{p2avg} = f_{p3avg}$ even though $b(k_{pk}/\omega_{pk}) = 1$. Theorem 17 was used to verify these results based on the steady-state gains of each plant and large steady-state gain of the 'PID'-controller, independent of the simulation. Fig. 3 confirms that the averaging power junction achieves consensus even though each plant (having the same steady-state gain) has different dynamic properties. In addition, we discover that the consensus power junction performs quite poorly in that the non-minimum 'like' phase properties result in $f_{p3con} = 0$ for most of the simulation Fig. 2 and Fig. 3. Fig. 4 indicates that the averaging power junction still

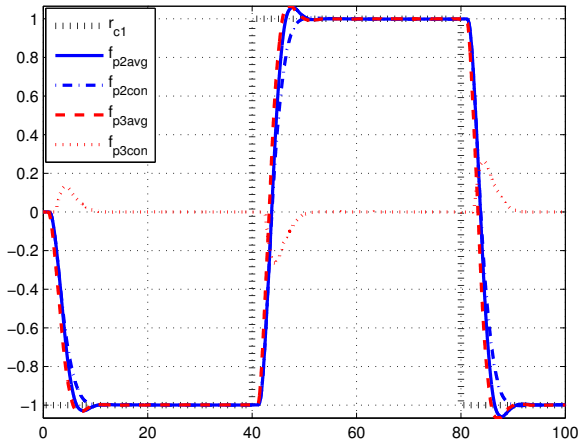

Fig. 3. Nominal velocity response $b = 1$, $i_p = 2$.

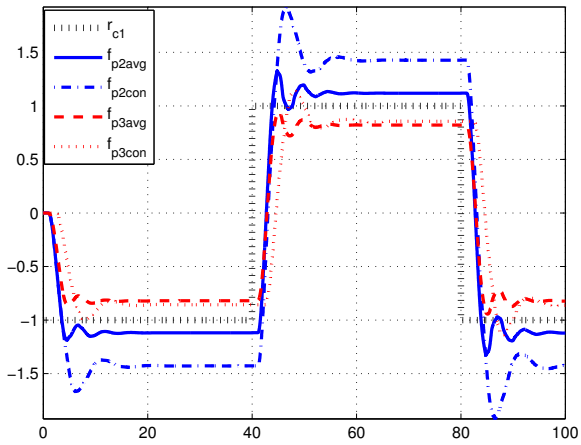

Fig. 4. Nominal velocity response $b = 2$, $i_p = 3$.

performs quite well in attempting to achieve a consensus in-spite a steady-state gain ratio of 5. By increasing b from 1 to 2 the consensus power junction was also able to achieve a better level of tracking than it could achieve when $b = 1$. Figs. 5, 6, 7 indicate that by increasing $b = 10$ tracking is improved for all cases, however, at the cost of increased over-shoot. The averaging power junction still vastly outperforms the consensus power junction.

3.2 Step Response with Identical Disturbances

In this section we perform the same set of simulations except that the following square-wave disturbance is introduced

$$r_{p2}(t) = r_{p3}(t) = -0.5\mathtt{sgn}(\sin 2\pi.025t). \qquad (40)$$

As expected, Figs. 8,9 indicate that the averaging power junction performs in a superior manner to the consensus power junction by rejecting most of the step disturbance input at steady state. Fig. 10 indicates that when the plants no longer have the same steady-state gain, the averaging power junction is still able to maintain its steady-state tracking error, while the consensus power junction tracking steady-state error is quite sensitive to the dis-

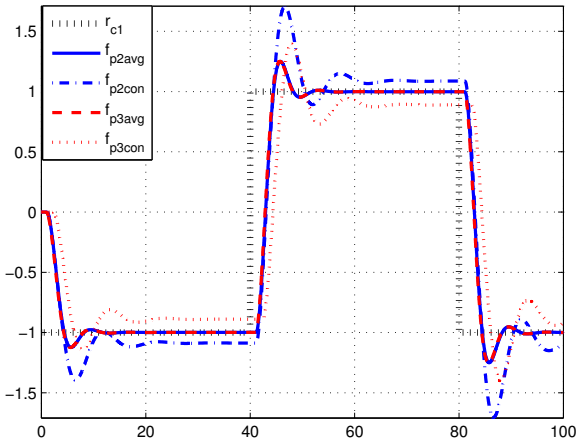

Fig. 5. Nominal velocity response $b = 10$, $i_p = 1$.

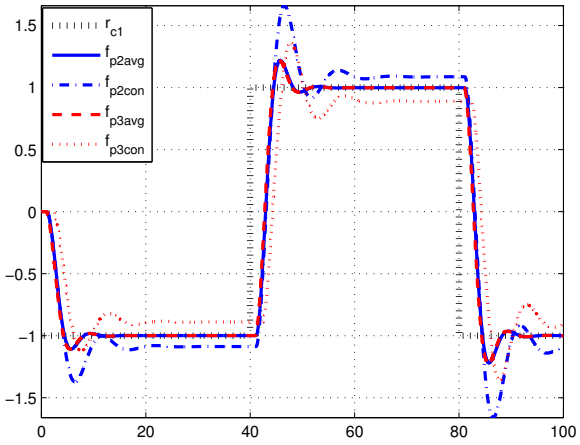

Fig. 6. Nominal velocity response $b = 10$, $i_p = 2$.

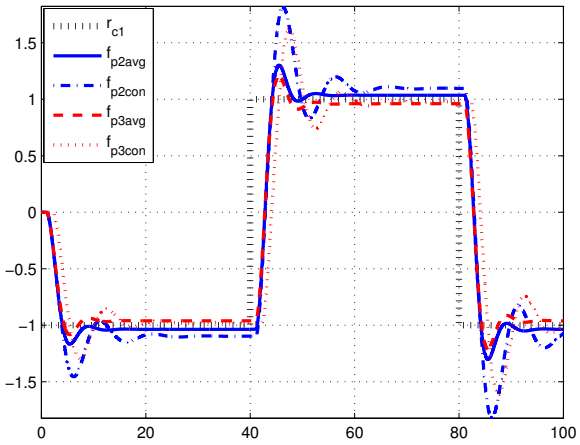

Fig. 7. Nominal velocity response $b = 10$, $i_p = 3$.

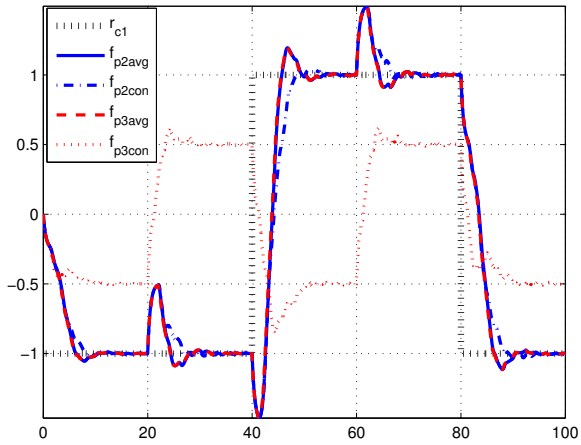

Fig. 8. Vel. response $b = 1$, $i_p = 1$, $r_{pk}(t)$ given by (40).

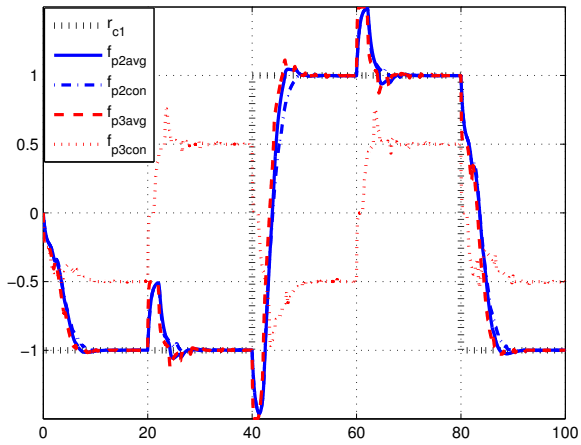

Fig. 9. Vel. response $b = 1$, $i_p = 2$, $r_{pk}(t)$ given by (40).

turbance when $b = 2$. Figs. 11,12,13 show overall improvement in disturbance rejection, and that the averaging power junction outperforms the consensus power junction.

3.3 Step Response with Opposite Disturbances

In this section we perform the same set of simulations except that the following square-wave disturbance is introduced

$$r_{p2}(t) = -r_{p3}(t) = 0.5\mathtt{sgn}(\sin 2\pi.025t). \qquad (41)$$

As expected, Figs. 14,15 indicate that the averaging power junction performs in a superior manner to the consensus power junction by rejecting most of the step disturbance input at steady state. There is a limit to how much disturbance rejection can be achieved for this case however. The 'PID'-controller can only split the difference between the two opposite disturbances in attempting to maintain the nominal set-point. This is the most extreme case of a bounded step-disturbance which can be applied to such a system. The 'PID'-controller, with the averaging power-junction can essentially reduce this difference in half when $b = 1$. Fig. 16 indicates that when the plants no longer have

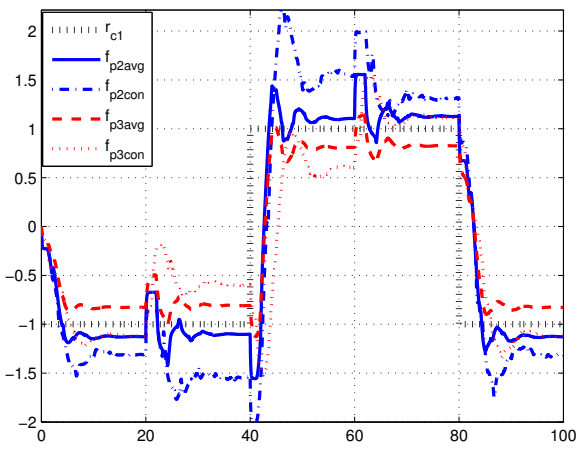

Fig. 10. Vel. response $b = 2$, $i_p = 3$, $r_{pk}(t)$ given by (40).

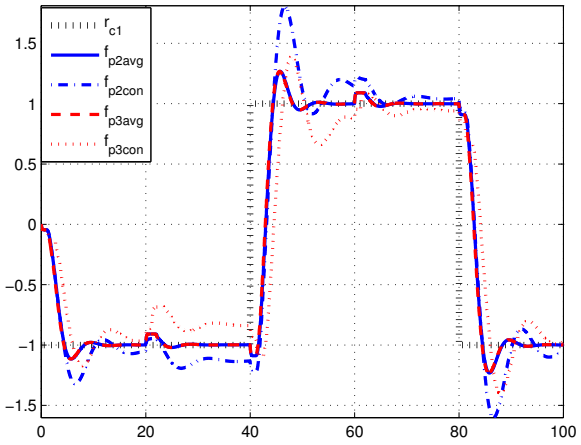

Fig. 11. Vel. response $b = 10$, $i_p = 1$, $r_{pk}(t)$ given by (40).

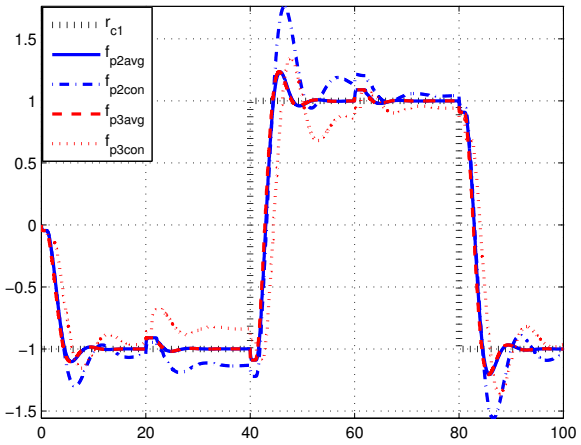

Fig. 12. Vel. response $b = 10$, $i_p = 2$, $r_{pk}(t)$ given by (40).

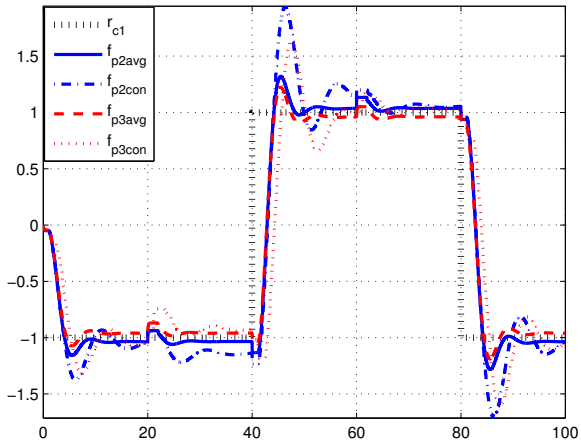

Fig. 13. Vel. response $b = 10$, $i_p = 3$, $r_{pk}(t)$ given by (40).

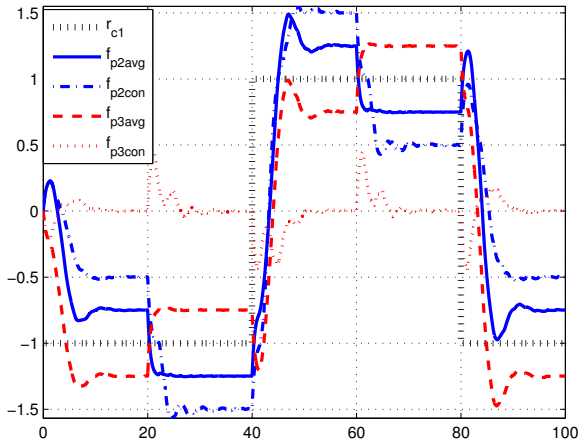

Fig. 14. Vel. response $b = 1$, $i_p = 1$, $r_{pk}(t)$ given by (41).

the same steady-state gain, the averaging power junction is still able to maintain a tighter steady-state tracking error than the consensus power junction tracking steady-state error when $b = 2$. Figs. 17,18,19 show overall improvement in disturbance rejection, and that the averaging power junction outperforms the consensus power junction.

4. CONCLUSIONS

A constructive method has been presented which allows the user to construct digital control networks in which passive plants can be interconnected in a manner such that L_2^m-stability is guaranteed. The PS and PH provide a bridge between the continuous time-domain to the discrete-time domain for the passive plants. The *IPES* and *ZOH* blocks provide a bridge between the discrete time-domain to the continuous-time domain for the passive digital controllers. The power-junction provides a general manner to interconnect many plants to many controllers. However, many different types of power-junctions can be implemented. We refined our averaging power junction which creates a highly parallel network. We also introduced a consensus power junction in which waves are interconnected in a series like manner in order to achieve

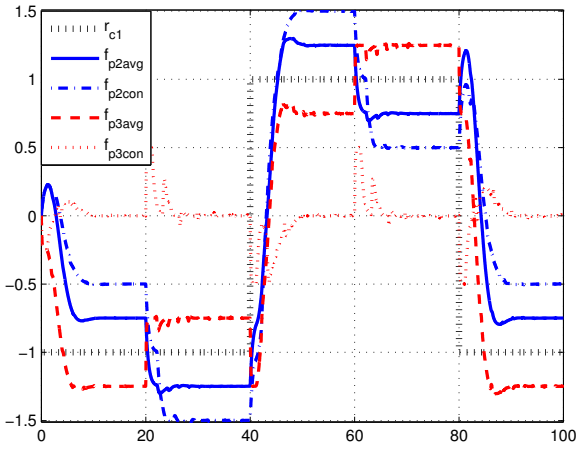

Fig. 15. Vel. response $b = 1$, $i_p = 2$, $r_{pk}(t)$ given by (41).

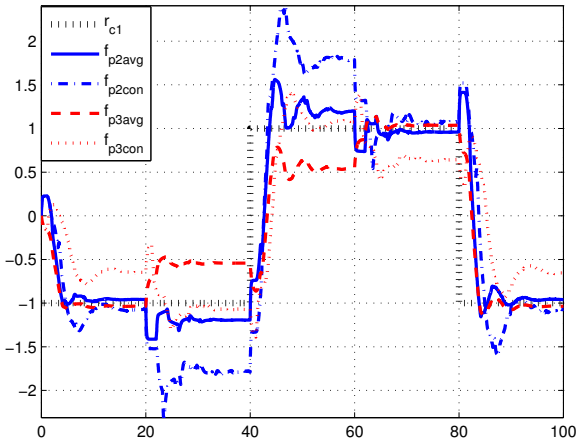

Fig. 16. Vel. response $b = 2$, $i_p = 3$, $r_{pk}(t)$ given by (41).

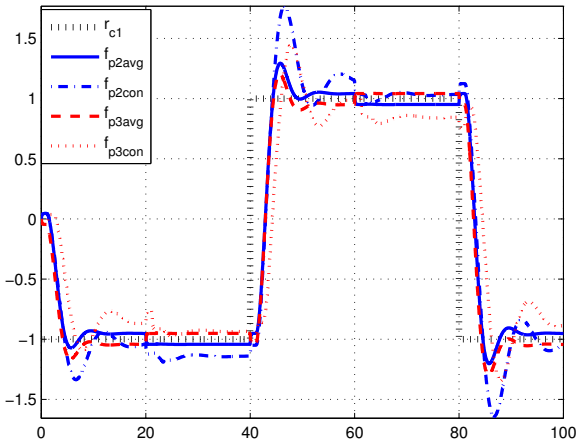

Fig. 17. Vel. response $b = 10$, $i_p = 1$, $r_{pk}(t)$ given by (41).

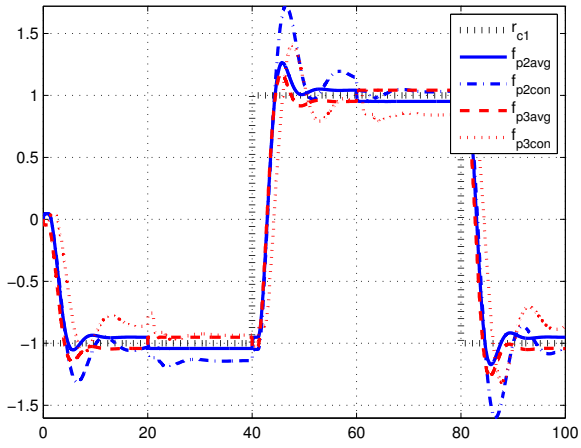

Fig. 18. Vel. response $b = 10$, $i_p = 2$, $r_{pk}(t)$ given by (41).

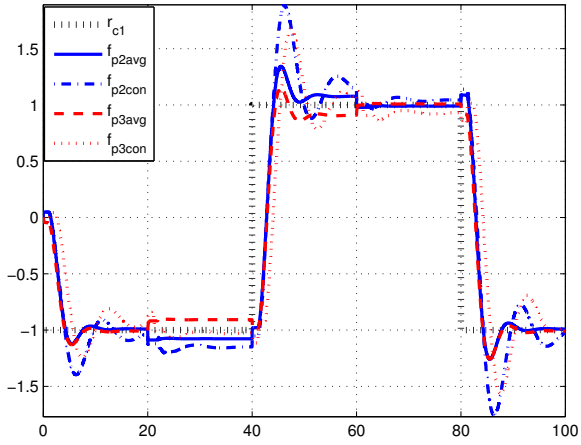

Fig. 19. Vel. response $b = 10$, $i_p = 3$, $r_{pk}(t)$ given by (41).

consensus. A steady-state analysis was performed for networks consisting of either an averaging power-junction or a consensus power-junction. The analysis for the averaging power-junction predicts consensus when the 'weaker-condition' that the steady-state gains for every plant must be the same, and the controllers steady-state gains must be large. For the consensus power-junction, consensus is only possible when all $bk_{pk} >> 1$ and $k_{cj} >> 1$, this outcome occurs for the averaging power-junction case as well. Simulation results verify our analysis and indicate that when a single digital 'PID' controller is used to control two linear plants, the averaging power junction out-performs the consensus power junction in achieving consensus and rejecting disturbances.

REFERENCES

Antsaklis, P. and Baillieul, J. (eds.) (2004). *Special Issue on Networked Control Systems*, volume 49 number 9 of *IEEE Transactions on Automatic Control*. IEEE.

Antsaklis, P. and Baillieul, J. (eds.) (2007). *Special Issue: Technology of Networked Control Systems*, volume 95 number 1 of *Proceedings of the IEEE*. IEEE.

Berestesky, P., Chopra, N., and Spong, M.W. (2004). Discrete time passivity in bilateral teleoperation over the internet. *Proceedings - IEEE International Conference on Robotics and Automation*, 2004(5), 4557 – 4564.

Breedveld, P.C. (2006). Port-based modeling of dynamic systems in terms of bond graphs. In I. Troch (ed.), *5th Vienna Symposium on Mathematical Modelling, Vienna*, volume ARGESIM Report no. 30, cd rom. ARGESIM and ASIM, Arbeitsgemeinschaft Simulation, Vienna.

Chopra, N. and Spong, M. (2006). Passivity-based control of multi-agent systems. *Advances in Robot Control: From Everyday Physics to Human-Like Movements*, 107–134.

Desoer, C.A. and Vidyasagar, M. (1975). *Feedback Systems: Input-Output Properties*. Academic Press, Inc., Orlando, FL, USA.

Fettweis, A. (1986). Wave digital filters: theory and practice. *Proceedings of the IEEE*, 74(2), 270 – 327.

Franklin, G.F., Powell, J.D., and Emami-Naeini, A. (2006). *Feedback Control of Dynamic Systems*. Prentice-Hall, 5th edition.

Golo, G., van der Schaft, A.J., Breedveld, P., and Maschke, B. (2003). Hamiltonian formulation of bond graphs. In *Nonlinear and Hybrid Systems in Automotive Control*, 351–372. Springer-Verlag, London, UK.

Haddad, W.M. and Chellaboina, V.S. (2008). *Nonlinear Dynamical Systems and Control: A Lyapunov-Based Approach*. Princeton University Press, Princeton, New Jersey, USA.

Kottenstette, N. and Antsaklis, P. (2007). Stable digital control networks for continuous passive plants subject to delays and data dropouts. *Decision and Control, 2007 46th IEEE Conference on*, 4433–4440. doi:10.1109/CDC.2007.4434752.

Kottenstette, N. and Antsaklis, P. (2008a). Control of multiple networked passive plants with delays and data dropouts. *American Control Conference, 2008*, 3126–3132. doi:10.1109/ACC.2008.4586973.

Kottenstette, N., Koutsoukos, X., Hall, J., Sztipanovits, J., and Antsaklis, P. (2008). Passivity-Based Design of Wireless Networked Control Systems for Robustness to Time-Varying Delays. *Real-Time Systems Symposium, 2008*, 15–24.

Kottenstette, N. and Antsaklis, P.J. (2008b). Wireless digital control of continuous passive plants over token ring networks. *International Journal of Robust and Nonlinear Control*. doi:10.1002/rnc.1395.

Kottenstette, N., Hall, J., Koutsoukos, X., Antsaklis, P., and Sztipanovits, J. (2009). Digital control of multiple discrete passive plants over networks. Technical Report ISIS-09-102, ISIS Vanderbilt.

Niemeyer, G. and Slotine, J.J.E. (2004). Telemanipulation with time delays. *International Journal of Robotics Research*, 23(9), 873 – 890. URL `http://dx.doi.org/10.1177/0278364904045563`.

Stramigioli, S., Secchi, C., van der Schaft, A.J., and Fantuzzi, C. (2005). Sampled data systems passivity and discrete port-hamiltonian systems. *IEEE Transactions on Robotics*, 21(4), 574 – 587. URL `http://dx.doi.org/10.1109/TRO.2004.842330`.

van der Schaft, A. (1999). *L2-Gain and Passivity in Nonlinear Control*. Springer-Verlag New York, Inc., Secaucus, NJ, USA.

Appendix A. *PASSIVE* SYSTEMS

The following is a brief summary on *passive* systems. The interested reader is referred to Desoer and Vidyasagar (1975); van der Schaft (1999); Haddad and Chellaboina (2008) for additional information. Let $\mathcal{T}$ represent a set indicating time in which $\mathcal{T} = \mathbb{R}^+$ for continuous time signals and $\mathcal{T} = \mathbb{Z}^+$ for discrete time signals. Let $\mathcal{V}$ be a linear space $\mathbb{R}^m$ and denote the space of all functions $u : \mathcal{T} \to \mathcal{V}$ by the symbol $\mathcal{H}$ which satisfy the following:

$$\|u\|_2^2 = \int_0^\infty u^\mathsf{T}(t)u(t)dt < \infty, \tag{A.1}$$

for continuous time systems (L_2^m), and

$$\|u\|_2^2 = \sum_0^\infty u^\mathsf{T}(i)u(i) < \infty, \tag{A.2}$$

for discrete time systems (l_2^m). Similarly we will denote the extended space of functions $u : \mathcal{T} \to \mathcal{V}$ in $\mathcal{H}_e$ which satisfy the following:

$$\|u_T\|_2^2 = \langle u, u\rangle_T = \int_0^T u^\mathsf{T}(t)u(t)dt < \infty;\ \forall T \in \mathcal{T} \tag{A.3}$$

for continuous time systems (L_{2e}^m), and

$$\|u_T\|_2^2 = \langle u, u\rangle_T = \sum_0^{T-1} u^\mathsf{T}(i)u(i) < \infty;\ \forall T \in \mathcal{T} \tag{A.4}$$

for discrete time systems (l_{2e}^m). Furthermore let $y = Hu$ describe a relationship of the function y to the function u in which the instantaneous output value at continuous time t is denoted $y(t) = Hu(t)$ and respectively $y(i) = Hu(i)$ at discrete time i.

Definition 20. A continuous time dynamic system $H : \mathcal{H}_e \to \mathcal{H}_e$ is L_2^m stable if

$$u \in L_2^m \implies Hu \in L_2^m. \tag{A.5}$$

Definition 21. A discrete time dynamic system $H : \mathcal{H}_e \to \mathcal{H}_e$ is l_2^m stable if

$$u \in l_2^m \implies Hu \in l_2^m. \tag{A.6}$$

Definition 22. Let $H : \mathcal{H}_e \to \mathcal{H}_e$. We say that H is

i) *passive* if $\exists \beta$ s.t.
$$\langle Hu, u\rangle_T \geq -\beta,\ \forall u \in \mathcal{H}_e,\ \forall T \in \mathcal{T} \tag{A.7}$$

ii) *strictly-input passive* if $\exists \delta > 0$ and $\exists \beta$ s.t.
$$\langle Hu, u\rangle_T \geq \delta\|u_T\|_2^2 - \beta,\ \forall u \in \mathcal{H}_e,\ \forall T \in \mathcal{T} \tag{A.8}$$

iii) *strictly-output passive* if $\exists \epsilon > 0$ and $\exists \beta$ s.t.
$$\langle Hu, u\rangle_T \geq \epsilon\|Hu_T\|_2^2 - \beta,\ \forall u \in \mathcal{H}_e,\ \forall T \in \mathcal{T} \tag{A.9}$$

iv) *non-expansive* if $\exists \hat{\gamma} > 0$ and $\exists \hat{\beta}$ s.t.
$$\|Hu_T\|_2^2 \leq \hat{\beta} + \hat{\gamma}^2\|u_T\|_2^2,\ \forall u \in \mathcal{H}_e,\ \forall T \in \mathcal{T} \tag{A.10}$$

Remark 1. A *non-expansive* system H is equivalent to any system which has finite L_2^m (l_2^m) gain in which there exists constants γ and β s.t. $0 < \gamma < \hat{\gamma}$ and satisfy

$$\|Hu_T\|_2 \leq \gamma\|u_T\|_2 + \beta,\ \forall u \in \mathcal{H}_e,\ \forall T \in \mathcal{T}. \tag{A.11}$$

Furthermore a *non-expansive* system implies L_2^m (l_2^m) stability (van der Schaft, 1999, p.4) ((Kottenstette and Antsaklis, 2007, Remark 1)).

Appendix B. ADDITIONAL PROOFS

B.1 Proof of Lemma 4

Proof. Revisiting left hand side of equation (9) and using the consensus power junction equations (12), (13) for the $n-m$ plants, we get

$$\sum_{k=m+1}^{n}(u_k^{\mathsf{T}}u_k - v_k^{\mathsf{T}}v_k) = u_n^{\mathsf{T}}u_n - v_m^{\mathsf{T}}v_m \tag{B.1}$$

Similarly, using the right hand side and using (10) and (11) yields

$$\sum_{j=1}^{m}(u_j^{\mathsf{T}}u_j - v_j^{\mathsf{T}}v_j) = u_1^{\mathsf{T}}u_1 - v_m^{\mathsf{T}}v_m \tag{B.2}$$

$$= u_n^{\mathsf{T}}u_n - v_m^{\mathsf{T}}v_m \tag{B.3}$$

From (B.1)and (B.2), it is evident that the power junction is lossless.

B.2 Proof of Lemma 10

Proof. Summing both sides of the power junction (9) with respect to the index $i \in \{1,\ldots,N-1\}$ results in

$$\sum_{k=m+1}^{n}\|(u_k)_N\|_2^2 - \|(v_k)_N\|_2^2 \geq \sum_{j=1}^{m}\|(u_j)_N\|_2^2 - \|(v_j)_N\|_2^2 \tag{B.4}$$

since the wave variable communication time-delays $c_j(i) = c_k(i) = d_u(i)$, $p_j(i) = p_k(i) = d_v(i)$ satisfy any of the conditions listed in Proposition 7 we proceed to substitute the right inequality from (20) with the right inequality of (B.4) which results in

$$\sum_{k=m+1}^{n}\|(u_k)_N\|_2^2 - \|(v_k)_N\|_2^2 \geq \sum_{j=1}^{m}\langle e_{cj}, f_{dpj}\rangle_N \tag{B.5}$$

and then proceed to substitute the left inequality from (19) with the left inequality of (B.5) which results in our desired inequality

$$\sum_{k=m+1}^{n}\langle f_{pk}, e_{dck}\rangle_{NT_s} \geq \sum_{j=1}^{m}\langle e_{cj}, f_{dpj}\rangle_N$$

which is (21).

B.3 Proof of Theorem 13

Proof. We recall from Lemma 10 that if any of the conditions listed in Proposition 7 are met for the wave variable communication time-delays $c_j(i) = c_k(i) = d_u(i)$, $p_j(i) = p_k(i) = d_v(i)$ that

$$\sum_{k=m+1}^{n}\langle f_{pk}(t), e_{dck}\rangle_{NT_s} \geq \sum_{j=1}^{m}\langle e_{cj}(i), f_{dpj}(i)\rangle_N \tag{B.6}$$

holds for all $N \geq 1$. We recall, that each *strictly-output passive* plant for $k \in \{m+1,\ldots,n\}$ satisfies

$$\langle f_{pk}, e_{pk}\rangle_{NT_s} \geq \epsilon_{pk}\|(f_{pk})_{NT_s}\|_2^2 - \beta_{pk} \tag{B.7}$$

while each *strictly-output passive* controller for $j \in \{1,\ldots,m\}$ satisfies (B.8).

$$\langle e_{cj}, f_{cj}\rangle_N \geq \epsilon_{cj}\|(e_{cj})_N\|_2^2 - \beta_{cj} \tag{B.8}$$

In addition, we can substitute (29) into (B.8) which yields

$$\langle e_{cj}, f_{cj}\rangle_N \geq \frac{\epsilon_{cj}}{T_s k_s^2}\|(e_{cj})_{NT_s}\|_2^2 - \beta_{cj}. \tag{B.9}$$

Substituting, $e_{dck} = r_{pk} - e_{pk}$ and $f_{dpj} = f_{cj} - r_{cj}$ into (B.6) yields

$$\sum_{k=m+1}^{n}\langle f_{pk}, r_{pk} - e_{pk}\rangle_{NT_s} \geq \sum_{j=1}^{m}\langle e_{cj}, f_{cj} - r_{cj}\rangle_N$$

which can be rewritten as

$$\sum_{k=m+1}^{n}\langle f_{pk}, r_{pk}\rangle_{NT_s} + \sum_{j=1}^{m}\langle e_{cj}, r_{cj}\rangle_N \geq \sum_{k=m+1}^{n}\langle f_{pk}, e_{pk}\rangle_{NT_s} + \sum_{j=1}^{m}\langle e_{cj}, f_{cj}\rangle_N \tag{B.10}$$

so that we can then substitute (B.7), (B.9), and (28) into (B.10) to yield

$$\sum_{k=m+1}^{n}\langle f_{pk}, r_{pk}\rangle_{NT_s} + \sum_{j=1}^{m}\langle e_{cj}, r_{cj}\rangle_{NT_s} \geq \epsilon[\sum_{k=m+1}^{n}\|(f_{pk})_{NT_s}\|_2^2 + \sum_{j=1}^{m}\|(e_{cj})_{NT_s}\|_2^2] - \beta \tag{B.11}$$

in which $\epsilon = \min(\epsilon_{pk}, \frac{\epsilon_{cj}}{T_s k_s^2})$, $k \in \{m+1,\ldots,n\}$ $j \in \{1,\ldots,m\}$ and $\beta = \sum_{k=m+1}^{n}\beta_{pk} + \sum_{j=1}^{m}\beta_{cj}$. Thus (B.11) satisfies Definition 22-iii for *strictly-output passivity* in which the input is the row vector of all controller and plant inputs $[r_{c1},\ldots,r_{cm},r_{p(m+1)},\ldots,r_{pn}]$, and the output is the row vector of all controller and plant outputs $[e_{c1},\ldots,e_{cm},f_{p(m+1)},\ldots,f_{pn}]$. When we let $\epsilon_{pk} = \epsilon_{cj} = 0$ we see that all the plants and controllers are *passive*, therefore the system depicted in Fig. 1 is *passive*.

B.4 Proof of Lemma 15

Proof. We recall the wave-equations for each plant:

$$u_{pk}(iT_s) = -v_{pk}(iT_s) + \sqrt{2b}f_{pk}(iT_s) \tag{B.12}$$

$$e_{dck}(iT_s) = -\sqrt{2b}v_{pk}(iT_s) + bf_{pk}(iT_s) \tag{B.13}$$

and the PS/PH steady state assumptions listed under Assumption 14:

$$u_{pk}(i) = \sqrt{T_s}u_{pk}(iT_s) \text{ and} \tag{B.14}$$

$$v_{pk}(iT_s) = \frac{v_{pk}(i)}{\sqrt{T_s}}. \tag{B.15}$$

Substituting the right hand side of (B.12) for $u_{pk}(iT_s)$ into (B.14) results in

$$u_{pk}(i) = \sqrt{T_s}\left(\sqrt{2b}f_{pk}(iT_s) - v_{pk}(iT_s)\right). \tag{B.16}$$

Proceeding to substitute the right hand side of (B.15) for $v_{pk}(iT_s)$ into (B.16) results in

$$u_{pk}(i) = \sqrt{2bT_s}f_{pk}(iT_s) - v_{pk}(i). \tag{B.17}$$

Substituting the right hand side of (B.15) for $v_{pk}(iT_s)$ into (B.13) results in

$$e_{dck}(iT_s) = bf_{pk}(iT_s) - \frac{\sqrt{2b}}{\sqrt{T_s}}v_{pk}(i). \tag{B.18}$$

Recalling that $e_{pk}(iT_s) = (r_{pk}(iT_s) - e_{dck}(iT_s))$ and the steady-state gain relationships for each plant we have

$$f_{pk}(iT_s) = k_{pk}(r_{pk}(iT_s) - e_{dck}(iT_s)). \tag{B.19}$$

Substituting the right hand side of (B.19) for $f_{pk}(iT_s)$ into (B.17) results in

$$u_{pk}(i) = \sqrt{2bT_s}k_{pk}(r_{pk}(iT_s) - e_{dck}(iT_s)) - v_{pk}(i). \quad \text{(B.20)}$$

Substituting the right hand side of (B.19) for $f_{pk}(iT_s)$ into (B.18) results in

$$e_{dck}(iT_s) = bk_{pk}(r_{pk}(iT_s) - e_{dck}(iT_s)) - \frac{\sqrt{2b}}{\sqrt{T_s}}v_{pk}(i). \quad \text{(B.21)}$$

Using (B.21) to solve for $e_{dck}(iT_s)$ results in

$$e_{dck}(i) = \frac{\sqrt{2b}}{\sqrt{T_s}(bk_{pk}+1)}v_{pk}(i) - \frac{bk_{pk}}{bk_{pk}+1}r_{pk}(iT_s) \quad \text{(B.22)}$$

Substituting the right hand side of (B.22) for $e_{dck}(i)$ into (B.20) and simplifying results in the solution for $u_{pk}(i)$

$$u_{pk}(i) = \frac{bk_{pk}-1}{bk_{pk}+1}v_{pk}(i) + \frac{\sqrt{2bT_s}k_{pk}}{bk_{pk}+1}r_{pk}(iT_s).$$

Likewise substituting the right hand side of (B.22) for $e_{dck}(i)$ into (B.19) results in the solution for $f_{pk}(iT_s)$

$$e_{pk}(iT_s) = \frac{\sqrt{2b}k_{pk}}{\sqrt{T_s}(bk_{pk}+1)}v_{pk}(i) + \frac{k_{pk}}{bk_{pk}+1}r_{pk}(iT_s).$$

B.5 Proof of Lemma 16

Proof. We recall the wave-equations for each controller:

$$v_{cj}(i) = u_{cj}(i) - \sqrt{\frac{2}{b}}e_{cj}(i) \quad \text{(B.23)}$$

$$f_{dpj}(i) = \sqrt{\frac{2}{b}}u_{cj}(i) - \frac{1}{b}e_{cj}(i) \quad \text{(B.24)}$$

and the relations which result from the *IPESH* steady state assumptions listed in Assumption 14:

$$r_{cj}(i) = -k_{sj}T_s r_{cj}(iT_s) \text{ and} \quad \text{(B.25)}$$

$$e_{cj}(iT_s) = -k_{sj}e_{cj}(i) \quad \text{(B.26)}$$

Recalling that $f_{cj}(i) = f_{dpj}(i) + r_{cj}(i)$ and substituting the right hand side of (B.25) for $r_{cj}(i)$ in our previous expression results in

$$f_{cj}(i) = f_{dpj}(i) - k_{sj}T_s r_{cj}(iT_s), \quad \text{(B.27)}$$

which allows us to compute the resulting steady state control effort,

$$e_{cj}(i) = k_{cj}(f_{dpj}(i) - k_{sj}T_s r_{cj}(iT_s)). \quad \text{(B.28)}$$

Substituting the right hand side of (B.28) for $e_{cj}(i)$ into (B.23) and (B.24) respectively results in the following equations:

$$v_{cj}(i) = u_{cj}(i) - \sqrt{\frac{2}{b}}k_{cj}(f_{dpj}(i) - k_{sj}T_s r_{cj}(iT_s)) \quad \text{(B.29)}$$

$$f_{dpj}(i) = \sqrt{\frac{2}{b}}u_{cj}(i) - \frac{k_{cj}}{b}(f_{dpj}(i) - k_{sj}T_s r_{cj}(iT_s)) \quad \text{(B.30)}$$

Solving (B.30) for $f_{dpj}(i)$ results in

$$f_{dpj}(i) = \frac{\sqrt{2b}}{k_{cj}+b}u_{cj}(i) + \frac{T_s k_{cj}k_{sj}}{k_{cj}+b}r_{cj}(iT_s) \quad \text{(B.31)}$$

Substituting the right hand side of (B.31) for $f_{dpj}(i)$ into (B.29) and simplifying results in our final expression for $v_{cj}(i)$

$$v_{cj}(i) = \frac{-k_{cj}+b}{k_{cj}+b}u_{cj}(i) + \frac{\sqrt{2b}T_s k_{cj}k_{sj}}{k_{cj}+b}r_{cj}(iT_s)$$

Likewise, substituting the right hand side of (B.31) for $f_{dpj}(i)$ into (B.28) results in

$$e_{cj}(i) = \frac{\sqrt{2b}k_{cj}}{k_{cj}+b}u_{cj}(i) - \frac{T_s bk_{cj}k_{sj}}{k_{cj}+b}r_{cj}(iT_s), \quad \text{(B.32)}$$

in which we substitute the right hand side of (B.32) for $e_{cj}(i)$ into (B.26) in order to derive our final expression for $e_{cj}(iT_s)$

$$e_{cj}(iT_s) = -\frac{\sqrt{2b}k_{cj}k_{sj}}{k_{cj}+b}u_{cj}(i) + \frac{T_s bk_{cj}k_{sj}^2}{k_{cj}+b}r_{cj}(iT_s).$$

B.6 Proof of Theorem B.6

Proof. For the case of a single controller and n-1 plants, the equations (34) and (36) can be rewritten as

$$\begin{aligned} u_{pk}(i) &= \alpha_k v_{pk}(i) + \gamma_k r_{pk}(iT_s) \\ v_{c1}(i) &= \beta_1 u_{c1}(i) + \beta_2 r_{c1}(iT_s) \end{aligned} \quad \text{(B.33)}$$

The properties of the consensus junction (12) imply that $v_{p2}(i) = v_{c1}(i)$. Exploiting this relationship in the above equations yields

$$\begin{aligned} u_{p2}(i) &= \alpha_2(\beta_1 u_{c1}(i) + \beta_2 r_{c1}(iT_s)) + \gamma_2 r_{p2}(iT_s) \\ &= \alpha_2\beta_1 u_{c1}(i) + \alpha_2\beta_2 r_{c1}(iT_s) + \gamma_2 r_{p2}(iT_s) \end{aligned} \quad \text{(B.34)}$$

However, for the cascaded plants (13), $v_3(i) = u_2(i)$. Thus, u_{p3} can be calculated as

$$\begin{aligned} &u_{p3}(i) = \alpha_3 v_3(iT_s) + \gamma_3 r_{p3}(iT_s) \\ &= \alpha_3(\alpha_2\beta_1 u_{c1}(i) + \alpha_2\beta_2 r_{c1}(iT_s) + \gamma_2 r_{p2}(iT_s)) + \gamma_3 r_{p3}(iT_s) \\ &= \alpha_3\alpha_2\beta_1 u_{c1}(i) + \alpha_3\alpha_2\beta_2 r_{c1}(iT_s) + \alpha_3\gamma_2 r_{p2}(iT_s)) \\ &\quad + \gamma_3 r_{p3}(iT_s) \end{aligned} \quad \text{(B.35)}$$

Observing the the above equations, recursively repeating them for the k^{th} plant leads to the first claim.

The consensus junction equations dictate that $u_{c1}(i) = u_{pn}(i)$. Hence,

$$\begin{aligned} u_{c1}(i) = &\left(\prod_{l=2}^{n}\alpha_l\right)\beta_1 u_{c1}(i) + \left(\prod_{l=2}^{n}\alpha_l\right)\beta_2 r_{c1}(iT_s) \\ &+ \sum_{l=2}^{n}\left(\prod_{s=l}^{n}\gamma_s\right)r_{pl}(iT_s) \end{aligned} \quad \text{(B.36)}$$

Solving the above equation demonstrates the second claim. For the case of a PI controller ($k_{c1} \to \infty$), under the assumption that $bk_{pk} >> 1$, $k_{s1} = \frac{1}{\sqrt{Ts}}$, and all disturbances equal zero, $\alpha_k = 1, \beta_1 = -1, \beta_2 = \sqrt{2bT_s}$. Thus, in steady state, $u_{c1}(i) = \sqrt{\frac{bT_s}{2}}$. As $u_{c1}(i) = u_{pn}(i)$, and from (34), $v_{pk}(i) = u_{c1}(i), \ \forall k$. Substituting in (34) yields that $f_{pk}(i) = r_{c1}(iTs) \ \forall k$.